Lipid hydration and mobility: An interplay between fluorescence solvent relaxation experiments and molecular dynamics simulations

P. Jurkiewicz[a], L. Cwiklik[a,b], P. Jungwirth[b], M. Hof[a,*]

[a] J. Heyrovský Institute of Physical Chemistry, Academy of Sciences of the Czech Republic, v. v. i., Dolejškova 3, 18223 Prague 8, Czech Republic

[b] Institute of Organic Chemistry and Biochemistry, Academy of Sciences of the Czech Republic and Center for Biomolecules and Complex Molecular Systems, Flemingovo nám. 2, 16610 Prague 6, Czech Republic

e-mails: piotr.jurkiewicz@jh-inst.cas.cz, lukasz.cwiklik@uochb.cas.cz, pavel.jungwirth@uochb.cas.cz, martin.hof@jh-inst.cas.cz

[*] Corresponding author. Tel. (+420)266053264, fax. (+420)286582307

Abstract

Fluorescence solvent relaxation experiments are based on the characterization of time-dependent shift in the fluorescence emission of a chromophore, yielding polarity and viscosity information of the chromophore immediate environment. Applied to phospholipid bilayers a defined location of the chromophore with respect to the z-axis of the bilayer allows monitoring of hydration and mobility of the probed segment of the lipid molecules. Specifically, time-resolved fluorescence experiments, fluorescence quenching data and molecular dynamic (MD) simulations show that 6-lauroyl-2-dimethylaminonaphthalene (Laurdan) reports on hydration and mobility of the *sn*-1 acyl groups in a phosphatidylcholine

bilayer. The time-dependent fluorescence shift (TDFS) of Laurdan reports on headgroup compression and expansion induced by the addition of different amounts of cationic lipids to phosphatidylcholine bilayers, which was predicted by previous MD simulations. Addition of truncated oxidized phospholipids leads to increased mobility and hydration at the *sn*-1 acyl level. That experimental finding can be explained by MD simulations, indicating that the truncated chains of the oxidized lipid molecules are looping back into aqueous phase, hence creating voids below the glycerol level. Fluorescence solvent relaxation experiments are also useful for the understanding of salt effects on the structure and dynamics of lipid bilayers. Those experiments for example demonstrate that large anions increase hydration and mobility at the *sn*-1 acyl level of phosphatidylcholine bilayers, which could not be explained by standard MD simulations. However, when introducing polarizability into the applied force field, those simulations show that big soft polarizable anions are able to interact with hydrophilic/hydrophobic interface of the lipid bilayer penetrating to the level probed by Laurdan and that they expand and destabilize the bilayer making it more hydrated and mobile.

Keywords:

sn-1 acyl group, Laurdan, oxidized phospholipids, DOTAP, Hofmeister, polarizability, transient Stokes shift

Abbreviations

MD – molecular dynamics, Laurdan – 6-lauroyl-2-dimethylaminonaphthalene, TDFS – time-dependent fluorescence shift, SR – solvent relaxation, Patman – 6-hexadecanoyl-2-(((2-(trimethylammonium)ethyl) methyl)amino)naphthalene chloride, Laurdan – 6-lauroyl-2-dimethylaminonaphthalene, Prodan – 6-propionyl-2-dimethylaminonaphthalene, Dtmac – 4-[(*n*-dodecylthio)methyl]-7-(*N*,*N*-dimethylamino)-coumarin, DOPC – 1,2-dioleoyl-*sn*-glycero-

3-phosphocholine, POPC – 1,2-palmitoyloleoyl-*sn*-glycero-3-phosphocholine, LUV – large unilamellar vesicle, DOTAP – 1,2-dioleoyl-3-trimethylammonium-propane, DMPC – 1,2-dimyristoyl-*sn*-glycero-3-phosphocholine, DMTAP – 1,2- dimyristoyl -3-trimethylammonium-propane, oxPL – oxidized lipid, POVPC – 1-palmitoyl-2-(5'-oxo-valeroyl)-sn-glycero-3-phosphocholine, PGPC – 1-palmitoyl-2-glutaryl-sn-glycero-3-phosphocholine, FCS – fluorescence correlation spectroscopy

1. Introduction

For rationalizing how a fluid biological membrane is functioning one has to know to what extent water is hydrating the different segments of the lipid molecules along the z-axis of the bilayer and how does this hydration influence the mobility of those segments. Historically, most of the information on such lipid hydration and mobility has been gained by NMR [1, 2], Neutron and X-ray diffraction [2, 3], and EPR experiments [4] on model membrane systems. Since the fluorescence emission of a chromophore may be strongly sensitive to the dynamics and polarity of his immediate vicinity, naturally also fluorescence experiments were performed to address hydration and mobility in lipid bilayers. Specifically, time-dependent fluorescence shift experiments (TDFS) of chromophores with a defined location with respect to the z-axis of a bilayer were shown to report changes in membrane hydration and mobility [5]. In this review we explain how the so-called solvent relaxation method (SR) can provide information on hydration and mobility of different lipid bilayer segments and demonstrate the validity of that information on three different examples: the impact on positively charged phospholipids, oxidized phospholipids and ions, respectively, on the hydration and mobility of the *sn*-1 carbonyl group of phosphatidylcholine bilayers. The conclusions drawn from time-dependent fluorescence experiments will be related to molecular dynamic (MD) simulations.

2.1 Fluorescence solvent relaxation experiments

Fluorescence solvent relaxation experiments or more precisely TDFS experiments are based on an ultrafast change in the dipole moment of the chromophore via electronic excitation, to which chromophore solvent shell must respond. This response of the immediate vicinity is reported by the time evolution of the frequency of maximum fluorescence, $\nu(t)$, which shifts to lower energies as the solvent shell relaxes to the dipole moment of the excited state of the chromophore. As shown for a large variety of neat liquids, the total amount of that TDFS, $\Delta\nu = \nu(0) - \nu(\infty)$, is directly proportional to the polarity of that solvent shell [6]. Since in lipid bilayers the polarity is predominantly determined by the presence of water, this parameter mirrors the hydration of chromophores environment within the bilayer. To characterize the kinetics of that relaxation process, $\nu(t)$ is normalized as follows:

$$C(t) = \frac{\nu(t) - \nu(\infty)}{\nu(0) - \nu(\infty)}.$$

C(t) describes the rearrangement kinetics of the immediate vicinity of the chromophore. C(t) can be fitted to one or – if necessary – more exponentials or numerically integrated to give a simple measure of the TDFS kinetics:

$$\tau = \int_0^\infty C(t)dt$$

Interestingly, water shows the fastest (among all liquids) and biphasic response to the perturbation by electronic excitation in an aromatic molecule: librational motions of water molecules occur within hundreds of fs, while the collective rearrangement of the water hydrogen bonding network occurs within a few ps [6]. The time scale of that reorientation kinetics changes dramatically when chromophore is incorporated within biomolecular assemblies. Specifically for biomembranes we have shown [7], that the TDFS of

chromophores located within the headgroup region of fluid bilayers is occurring in some cases exclusively of the ns time scale. Keeping in mind that bulk water is responding about 1000 times faster, we intuitively interpreted the observed ns TDFS as phospholipid headgroup dynamics [8]. On the other hand, certain membrane probe molecules report that beside of such a ns relaxation process, a part of the TDFS is occurring on the ps time scale [7]. Since the chemical structure of those probes and experimental data indicate that those chromophores are located in the external interphase of the bilayer, we suggested that within the ensemble of those dye molecules two populations of chromophore location exist. One population reports the above-mentioned ns headgroup dynamics, and the other population the fast bulk water response [7]. The interpretation of the reported nanosecond TDFS as reorientation kinetics of water molecules bound to functional groups of the lipid molecules, finds its support from analogous experiments and molecular dynamics simulations of TDFS in proteins. Although in this context the misleading term “biological water” was introduced and connected with the process of water molecules exchanging between the bulk and bound state [9], MD simulations by Halle showed that the interpretation of TDFS in term of bound and bulk water, although being simple, describes the experimental data in proteins well [10]. From these simulations it became clear that TDFS can report on the dynamics of hydrated functional groups within a protein, but not on the exchange process of individual water molecules [11].

2.2. Location of the chromophores within the lipid bilayer

Following the argumentation above TDFS of chromophores in membranes may report on the rearrangement response of the hydrated functional groups of lipid molecules as well as on the level of hydration within the bilayer. Keeping in mind the extreme anisotropy of a lipid bilayer along the z-axis in terms of hydration and mobility [12] a defined positioning of the

respective chromophore along that z-axis is the main requirement for a valuable application of the fluorescence solvent relaxation method. In this context we have used a series of amphiphilic compounds, the chromophore of which is reporting on the hydration and mobility of a certain lipid segment along the z-axis of the bilayer. The majority of those dyes and their location along the *z*-axis of a phospholipid bilayer are depicted in Figure 2 of Jurkiewicz et al 2005 [5]. Within the frame of this review, we will focus on four compounds, the chromophore of which is located within the headgroup region (Fig. 1): 6-hexadecanoyl-2-(((2-(trimethylammonium)ethyl) methyl)amino)naphthalene chloride (Patman) and 6-lauroyl-2-dimethylaminonaphthalene (Laurdan) are located at the level of *sn*-1 carbonyl, the latter being about 0.1 nm closer to the membrane/water interface [12]. The average location of 6-propionyl-2-dimethylaminonaphthalene (Prodan) which has the same chromophore as Patman and Laurdan, is further shifted towards that interface, but much less defined. 4-[(*n*-dodecylthio)methyl]-7-(*N*,*N*-dimethylamino)-coumarin (Dtmac) has a different chromophore, but in a rather defined localization between the *sn*-2 carbonyl and the phosphate group [13]. The location of those chromophores was estimated at first by the so-called parallax fluorescence quenching experiments [14]. Further information on „what segment those chromophores are probing“ were obtained by TDFS and quenching experiments using phosptatidylcholines with different hydrocarbon chains [12] and molecular dynamic simulations, the results of the latter will be discussed later in this review.

Because of the polarity/hydration profile of lipid membranes [15] and the fact that the total TDFS, $\Delta\nu$ (for a given chromophore) is proportionally to the polarity of the immediate environment of the chromophore [6] it becomes smaller when approaching the non-hydrated bilayer interior. Notably, values of $\Delta\nu$ for all four probes in POPC LUVs (10°C) were approx. equal: 2100, 4300, 3950, and 3350 cm^{-1} for Dtmac (different chromophore!), Prodan, Laurdan, and Patman, respectively. The values obtained for τ in POPC reflecting the probed

mobility of the chromophore environment were as follows: Dtmac 1.17, Prodan 2.1, Laurdan 3.12, and Patman 4.15 ns. In summary, this data shows that TDFS of those well defined located dyes demonstrates a distinct hydration and mobility decrease when "moving" from the phosphate region towards the carbonyl groups of the bilayer. In terms of probing headgroup hydration and mobility, this data together with the determined location of the chromophores confirm that $\Delta\nu$ and τ obtained using Laurdan and Patman report on hydration and mobility of the *sn*-1 acyl group, respectively. TDFS reported by Dtmac, on the other hand, should provide equivalent information about the phosphate level. In the next sections we will concentrate on SR measurements using Laurdan and will relate them to the results obtained from MD simulations.

3. MD addressing fluorescent probes in lipid bilayers

3.1. Membrane location of Laurdan in its ground and excited state

Although locations of such fluorescent probes as Laurdan or Patman in phospholipid bilayer have been determined using (parallax) quenching with spin-labeled lipids [12], a few open questions remained, namely the width of the fluorophore distribution and its possible relocation upon excitation. To address them, ground and excited states configurations of Prodan and Laurdan in vacuum were calculated using quantum mechanics and then were used in all-atom classical MD simulations of DOPC bilayer [16]. First, a spontaneous adsorption and incorporation of the dyes into the membrane was observed and then the distributions of the location of the fluorophores were calculated. At a certain point, after over 100 ns, the fluorophores were "excited" by simply replacing their ground state structures with the ones calculated for their first excited states and their trajectories were further analyzed for 100 ns.

This simple procedure allowed determination of Laurdan location and answering the question of possible dye relocation upon electronic excitation. The distributions obtained for Laurdan using MD together with the results of quenching experiments are presented in Fig. 2. The calculated mean distances of Laurdan fluorophore from DOPC bilayer center of (12.3 ± 2.1) Å and (13.5 ± 2.5) Å, for ground and excited states, respectively, are in good agreement with the value of (11.4 ± 2.0) Å measured using parallax method. In the quenching experiments it was observed that the location obtained depends at what emission wavelength the fluorescence intensity was measured. Shorter wavelengths were emitted by deeper located fluorophore molecules, while longer, red-shifted, emission occurred from fluorophores located closer to the water interface; i.e. the values of 9.9 Å and 12.0 Å were obtained for emission at 420 nm and 530 nm, respectively. Since, the emission of Laurdan is strongly red-shifting in time after the excitation it was hypothesized that Laurdan fluorophore is moving toward water phase, while in excited state. This was confirmed by the MD simulations, which showed shifted and slightly broadened location histogram for the S1 state. One has to keep in mind that the effective histogram of Laurdan location in S1 state would be much less shifted than the one calculated here from 100 ns trajectory, due to limited fluorescence lifetime (about 4 ns in our experiments), after which the dye goes back to S0 configuration and most probably deepens in the bilayer again.

3.2. Estimating timescale of relaxation probed by Laurdan

Computer simulations of solvent relaxation in neat solvent are known to be a valuable tool in understanding of relaxation kinetics on a molecular level, see e.g. [17, 18]. The treatment described in section 3.1. together with continuously increasing computer power allows application of MD to study relaxation in model lipid membranes. Fluorescence solvent

relaxation response was estimated from the reorientation of the dipoles of fluorescent probe and water molecules. The dipole vector of the fluorophore and the dipole vectors of water molecules in its closest vicinity tend to orient antiparallel. Thus, examination of the angle between Laurdan dipole vector and the mean vector of the solvating water gives a satisfactory measure of dipolar relaxation. Such analysis was performed for Laurdan molecule in pure water and in DOPC bilayer. The results are summarized in Fig. 3. in a form of time-space evolution of the scalar product of the two above mentioned vectors. It is apparent that relaxations in those two environments occur on entirely different timescales. While pure water relaxes within a few picoseconds, relaxation in DOPC takes nanoseconds; moreover it is clearly two-componential. Majority of the relaxation in the lipid bilayer at room temperature completes within 0.5 ns, but there is also a long tail that reaches up to 4 ns. Another difference is that in DOPC excitation of Laurdan affects water molecules distanced as far as 3-12 Å from its fluorophore, while in water only the closest 2-3 Å of the bulk are affected. In addition to being in agreement with the picoseconds and nanosecond time-scales of the TDFS measured in water and in lipid bilayer, respectively, the MD results allow correlation of the observed relaxation with molecular mobility. In the bulk water a substantial part of relaxation is due to rotation of water and consequently is proportional to the viscosity of the solvent. In lipid bilayer below glycerol level, where Laurdan is located, water molecules are sparse and fully bound to lipids (mainly to lipid carbonyls). This is why we consider mobility of hydrated lipid moieties (mostly carbonyls in the case of Laurdan), to be influencing the measured solvent relaxation kinetics. Nanosecond relaxation time carries information exclusively about mobility of hydrated lipids at the level where the probe is located and not about dynamics of water molecules, which interchange or even exchange with those from bulk water on a picosecond timescale (unpublished MD results and [1]).

4. Comparing TDFS and MD results – case study

Computer simulations greatly contributed to understanding of solvation dynamics in neat solvents [19]. As we have demonstrated in the previous section, MD simulations considerably advanced our understanding of the origin of the measured TDFS in lipid bilayers. It is known that MD simulations can be performed (in the absence of a chromophores) to rationalize changes in lipid bilayer organization induced e.g. by positively charged phospholipids, oxidized phospholipids and salt solutions, on atomistic level. Moreover, such MD simulations can reveal parameters which do have a direct impact on hydration and mobility and, thus, can be linked to the measured TDFS parameters, i.e. total emission shift, $\Delta\nu$, and mean relaxation time, τ. Below we give a few examples of studies were TDFS and MD were effectively combined and we discuss the coupling between the two techniques.

4.1. Cationic / zwitterionic lipid bilayer

Synthetic cationic lipids, like 1,2-dioleoyl-3-trimethylammonium-propane (DOTAP), are used for delivery of nucleic acids into living organisms and were one of the first promising non-viral vectors for gene therapy [20]. This motivated numerous fundamental studies of structure and properties of cationic lipid bilayers [21]. A nonideal mixing of TAP and PC and the PC headgroup rearrangement was first shown using ^{2}H NMR and DSC techniques [22, 23]. More recently, Gurtovenko et al. have simulated mixture of DMPC/DMTAP (1,2-dimyristoyl-*sn*-glycero-3-phosphocholine/1,2- dimyristoyl -3-trimethylammonium-propane) [24]. Their MD simulations illustrated the rise of DMPC headgroup dipoles upon addition of DMTAP; see Fig. 4. These were electrostatic interactions

between cationic TAP headgroup and PC dipole that led to the headgroup rearrangement and consequently to membrane compression up to $\chi = 0.5$; χ being the mole fraction of DMTAP. Further increase of DMATP content led back to membrane expansion due to TAP-TAP repulsion. The effect was adequately illustrated by the mean area per lipid as a function of DMTAP content; reproduced in Fig. 4.

While studying analogous mixture of DOPC and DOTAP with solvent relaxation technique we found similar non-monotonic dependence of relaxation time, τ, measured for Laurdan [12]. Relaxation time exhibited pronounced maximum at χ=0.3, which means that the mobility of lipids at the carbonyls, where Laurdan is located, was there the most restricted, see Fig. 4. The relation between τ and $\langle A \rangle$ is here rather intuitive: the more compressed the bilayer, smaller $\langle A \rangle$, the more restricted mobility of lipids, longer τ. This is a general dependence that is often and successfully used. But it holds true under one important assumption that the fluorescent probe of mobility is located at the depth level where the lateral pressure controls the area of membrane. In other words, if the area per lipid is not affected by something that is located at a different level than the fluorophore and thus can not be probed. In our example DOPC/DOTAP mixture has considerably bulkier aliphatic backbone (two oleic chains instead of two fully saturated myristic chains in the case of DMPC/DMTAP), which is likely to limit bilayer compression even when the rearrangement of the headgroup region allows for it. This is likely the cause of the fact that the maximum of τ for DOPC/DOTAP is at $\chi = 0.3$ and the minimum of $\langle A \rangle$ for DMPC/DMTAP at $\chi = 0.5$. This hypothesis has been later confirmed by measuring TDFS in DMPC/DMTAP mixture, where the maximum was observed at $\chi = 0.45$, being in much better agreement with the MD results; see Fig. 4 and [25] for details.

4.2. Oxidized lipid bilayer

Oxidized lipids (oxPLs) are natural products of polyunsaturated lipids that underwent an oxidative stress. Since their presence has been linked with many diseases, their properties are extensively studied [26]. One of the pathways of oxidation leads to truncation of the *sn*-1 chain of a phospholipid. The truncated lipid has conical geometry, which might influence physical properties of oxidized lipid bilayer [27].

We have performed combined SR and MD studies on POPC lipid bilayer, in which 10 mol% of lipid molecules was substituted with one of two oxidized lipids: 1-palmitoyl-2-(5'-oxo-valeroyl)-sn-glycero-3-phosphocholine (POVPC) or 1-palmitoyl-2-glutaryl-sn-glycero-3-phosphocholine (PGPC); both molecules are analogues of POPC with *sn*-2 chain truncated at 5^{th} carbon, where carboxyl or aldehyde group is introduced, respectively. TDFS measurements performed using Laurdan revealed significant changes in both SR parameters. First, relaxation kinetics described by τ is faster when oxPLs are present – carbonyl level probed by Laurdan is much more mobile. We might expect then, that the area per lipid calculated from MD is increased. This is however not the case. On the contrary $\langle A \rangle = 0.66$ nm^2 for pure POPC drops to $\langle A \rangle = 0.61$ nm^2 for 10 mol% of PGPC; while the value of τ is decreasing from 4.05 ns to 3.85 ns, respectively. So the membrane becomes laterally compressed, while Laurdan senses increased mobility. The explanation of this apparent discrepancy can be easily obtained from MD, when noticing that the truncated carboxylic chains of PGPC molecules are looping back into aqueous phase, hence creating voids below the glycerol level. Those voids cause compression of the membrane ($\langle A \rangle$ decreases), although the compression is limited by the headgroup region now incorporating also the truncated chains. In consequence, Laurdan has still much more space at its location and this is why it senses higher mobility there.

Analysis of the bilayer structure provided using MD, namely distributions of the positions of the truncated chains of the oxPLs, helped us in understanding molecular basis of the differences between local mobility probed by Laurdan and lateral diffusion of lipids that was also measured using fluorescence correlation spectroscopy (FCS) [28]. We refer the reader to the original paper for details [29].

Laurdan sensed also an increased hydration in lipid bilayers containing oxidized lipids. This was particularly noticeable in the case of POVPC, for which $\Delta\nu$ increased to 3900 cm^{-1} from 3750 cm^{-1} measured for pure POPC. To approach the question of membrane hydration using MD, mean numbers of water molecules in different locations in membrane were calculated. An increased number of water molecules was found within 0.5 nm radius from *sn*-1 carbonyl of lipids in POVPC-containing membrane. This agrees with the result of SR measurements and provides another evidence of the location of Laurdan fluorophore near *sn*-1 carbonyl.

4.3. Ions in lipid membranes

Ionic effects certainly play an important role in membrane biology and numerous specific salt effects on structure and dynamics of lipid bilayer have been observed since the discovery of the Hofmeister series [30]. We have studied influence of different monovalent cations and anions on hydration, mobility, and other parameters of neutral phospholipid bilayers using SR and MD trying to keep the same as many conditions of experiment and simulations as possible.

The first important finding was that sodium ions strongly adhere to DOPC bilayer, which can be verified in MD [31]. They slow down mobility at the carbonyl level probed by Laurdan: τ = 0.56 ns for water and 1.45 ns for 1M NaCl, which is accompanied by reduction

of <*A*> from 0.72 nm^2 to 0.69 nm^2. Moreover, lateral diffusion of lipids was studied experimentally (FCS) and in MD. Although both the methods reported reduced lateral mobility, the changes were close to the error. Studying dynamical properties of big complex ensembles of molecules is difficult in all-atom MD and the uncertainty of the obtained values is often high. This is why we are usually limited to compare SR kinetics with the area per lipid from MD.

Specific effects of monovalent anions are stronger than those of cations, and both SR parameters, τ and $\Delta\nu$ are sensitive to them [32]. The obtained results follow the Hofmeister series in the form: NaCl < NaBr < NaI < $NaClO_4$ < NaSCN. NaCl, as it was shown, slows down relaxation probed by Laurdan in DOPC. NaSCN on the other hand speeds it up significantly and increases total spectral shift, $\Delta\nu$. Apparently, thiocyanate anion disturbs DOPC bilayer considerably expanding it. It was known that for big soft anions polarizability is likely to be a key factor for their interaction with phospholipid bilayer. Since MD simulations of big thiocyanate using polarizable force-field would be very time consuming, NaI was simulated instead. It was shown that I^- penetrates deep into DOPC bilayer reaching the glycerol level. That deep location was not observed in MD simulations, in which polarizability was excluded. It showed that big soft polarizable anions are able to interact with hydrophilic/hydrophobic interface of the lipid bilayer penetrating to the level probed by Laurdan and that they expand and destabilize the bilayer making it more hydrated and mobile.

5. Conclusions

1. SR and MD are complementary methods that are able to elucidate hydration and packing effects in model lipid membranes on a molecular level.

2. SR and MD both profit from this combination. SR gains a tool to illustrate the studied phenomena and more importantly to test the hypotheses produced on the basis of SR results. MD gains another method for experimental validation of MD predictions that measures parameters difficult to obtain with other experimental methods.

3. SR also became much more defined and better understood method thanks to the application of MD to characterize location of the probes and to simulate dynamics of water and lipids in the vicinity of the fluorophore.

4. When compared to NMR, Neutron and X-ray diffraction, and EPR experiments, fluorescence experiments can be much easier expanded to more realistic model membranes or even to cell membranes, which defines the future potential of the solvent relaxation in biomembrane research.

6. Acknowledgements

The authors acknowledges support from the Czech Ministry of Education (grant LC 512 (Pavel J.) and LC 06063 (M.H.)), the Czech Science Foundation (grants 203/08/0114 and EUROMEMBRANES project MEM/09/E006), and the Academy of Sciences (Praemium Academie; Pavel J.).

7. References

[1] Westlund P.O., Line shape analysis of NMR powder spectra of (H2O)-H-2 in lipid bilayer systems, J. Phys. Chem. B 104 (2000) 6059-6064.
[2] Gawrisch K., Gaede H.C., Mihailescu M., White S.H., Hydration of POPC bilayers studied by H-1-PFG-MAS-NOESY and neutron diffraction, Eur. Biophys. J. Biophys. Lett. 36 (2007) 281-291.
[3] Tristram-Nagle S., Nagle J.F., Lipid bilayers: thermodynamics, structure, fluctuations, and interactions, Chem. Phys. Lipids 127 (2004) 3-14.
[4] Marsh D., Polarity and permeation profiles in lipid membranes, Proc. Natl. Acad. Sci. U. S. A. 98 (2001) 7777-7782.
[5] Jurkiewicz P., Sykora J., Olzynska A., Humplickova J., Hof M., Solvent relaxation in phospholipid bilayers: Principles and recent applications, J. Fluoresc. 15 (2005) 883-894.

[6] Horng M.L., Gardecki J.A., Papazyan A., Maroncelli M., Subpicosecond Measurements of Polar Solvation Dynamics - Coumarin-153 Revisited, J Phys Chem-Us 99 (1995) 17311-17337.
[7] Sykora J., Kapusta P., Fidler V., Hof M., On what time scale does solvent relaxation in phospholipid bilayers happen?, Langmuir 18 (2002) 571-574.
[8] Hutterer R., Schneider F.W., Sprinz H., Hof M., Binding and relaxation behaviour of Prodan and Patman in phospholipid vesicles: A fluorescence and H-1 NMR study, Biophys Chem 61 (1996) 151-160.
[9] Pal S.K., Peon J., Bagchi B., Zewail A.H., Biological water: Femtosecond dynamics of macromolecular hydration, J. Phys. Chem. B 106 (2002) 12376-12395.
[10] Halle B., Nilsson L., Does the Dynamic Stokes Shift Report on Slow Protein Hydration Dynamics?, J. Phys. Chem. B 113 (2009) 8210-8213.
[11] Peon J., Pal S.K., Zewail A.H., Hydration at the surface of the protein Monellin: Dynamics with femtosecond resolution, Proc. Natl. Acad. Sci. U. S. A. 99 (2002) 10964-10969.
[12] Jurkiewicz P., Olzynska A., Langner M., Hof M., Headgroup hydration and mobility of DOTAP/DOPC bilayers: A fluorescence solvent relaxation study, Langmuir 22 (2006) 8741-8749.
[13] Sykora J., Jurkiewicz P., Epand R.M., Kraayenhof R., Langner M., Hof M., Influence of the curvature on the water structure in the headgroup region of phospholipid bilayer studied by the solvent relaxation technique, Chem. Phys. Lipids 135 (2005) 213-221.
[14] Chattopadhyay A., London E., Parallax Method for Direct Measurement of Membrane Penetration Depth Utilizing Fluorescence Quenching by Spin-Labeled Phospholipids, Biochemistry-Us 26 (1987) 39-45.
[15] Nagle J.F., Tristram-Nagle S., Structure of lipid bilayers, Biochim. Biophys. Acta-Rev. Biomembr. 1469 (2000) 159-195.
[16] Barucha-Kraszewska J., Kraszewski S., Jurkiewicz P., Ramseyer C., Hof M., Numerical studies of the membrane fluorescent dyes dynamics in ground and excited states, Biochim. Biophys. Acta-Biomembr. 1798 (2010) 1724-1734.
[17] Jimenez R., Fleming G.R., Kumar P.V., Maroncelli M., Femtosecond solvation dynamics of water, Nature 369 (1994) 471-473.
[18] Perera L., Berkowitz M.L., Solvation dynamics in a Stockmayer fluid, in: Blum L. and Malik F.B. (Eds.), Condensed Matter Theories, Vol 8, Plenum Press Div Plenum Publishing Corp, New York, 1993, pp. 461-483.
[19] Stratt R.M., Maroncelli M., Nonreactive dynamics in solution: The emerging molecular view of solvation dynamics and vibrational relaxation, J Phys Chem-Us 100 (1996) 12981-12996.
[20] Felgner P.L., Gadek T.R., Holm M., Roman R., Chan H.W., Wenz M., Northrop J.P., Ringold G.M., Danielsen M., LIPOFECTION - A HIGHLY EFFICIENT, LIPID-MEDIATED DNA-TRANSFECTION PROCEDURE, Proc. Natl. Acad. Sci. U. S. A. 84 (1987) 7413-7417.
[21] Simberg D., Weisman S., Talmon Y., Barenholz Y., DOTAP (and other cationic lipids): Chemistry, biophysics, and transfection, Crit. Rev. Ther. Drug Carr. Syst. 21 (2004) 257-317.
[22] Scherer P.G., Seelig J., Electric charge effects on phospholipid headgroups - phosphatidylcholine in mixtures with cationic and anionic aphiphilles, Biochemistry-Us 28 (1989) 7720-7728.
[23] Silvius J.R., Anomalous mixing of zwitterionic and anionic phospholipids with double-chain cationic amphiphiles in lipid bilayers, Biochimica Et Biophysica Acta 1070 (1991) 51-59.

[24] Gurtovenko A.A., Patra M., Karttunen M., Vattulainen I., Cationic DMPC/DMTAP lipid bilayers: Molecular dynamics study, Biophys. J. 86 (2004) 3461-3472.
[25] Olzynska A., Jurkiewicz P., Hof M., Properties of mixed cationic membranes studied by fluorescence solvent relaxation, J. Fluoresc. 18 (2008) 925-928.
[26] Fruhwirth G.O., Loidl A., Hermetter A., Oxidized phospholipids: From molecular properties to disease, Biochim. Biophys. Acta-Mol. Basis Dis. 1772 (2007) 718-736.
[27] Pande A.H., Kar S., Tripathy R.K., Oxidatively modified fatty acyl chain determines physicochemical properties of aggregates of oxidized phospholipids, Biochim. Biophys. Acta-Biomembr. 1798 442-452.
[28] Machan R., Hof M., Lipid diffusion in planar membranes investigated by fluorescence correlation spectroscopy, Biochim. Biophys. Acta-Biomembr. 1798 (2010) 1377-1391.
[29] Beranova L., Cwiklik L., Jurkiewicz P., Hof M., Jungwirth P., Oxidation Changes Physical Properties of Phospholipid Bilayers: Fluorescence Spectroscopy and Molecular Simulations, Langmuir 26 (2010) 6140-6144.
[30] Kunz W., Lo Nostro P., Ninham B.W., The present state of affairs with Hofffieister effects, Curr. Opin. Colloid Interface Sci. 9 (2004) 1-18.
[31] Vacha R., Siu S.W.I., Petrov M., Bockmann R.A., Barucha-Kraszewska J., Jurkiewicz P., Hof M., Berkowitz M.L., Jungwirth P., Effects of Alkali Cations and Halide Anions on the DOPC Lipid Membrane, J. Phys. Chem. A 113 (2009) 7235-7243.
[32] Vacha R., Jurkiewicz P., Petrov M., Berkowitz M.L., Bockmann R.A., Barucha-Kraszewska J., Hof M., Jungwirth P., Mechanism of Interaction of Monovalent Ions with Phosphatidylcholine Lipid Membranes, J. Phys. Chem. B 114 (2010) 9504-9509.

Fig. 1. Chemical structures of the probes included in the DOPC bilayer depicting their approximate location. Patman, Laurdan and Prodan do have identical chromophores and accordingly the derived $\Delta\nu$ values are comparable among them.

Fig. 2. Location of the fluorophore of Laurdan along DOPC bilayer normal. The distribution histograms were calculated from MD trajectories of 73 ns for ground S0 state and 100 ns for S1 excited states, respectively [16]. Histogram envelopes are best multi-Gaussian fits, with 2 and 4 components for S0 and S1, respectively. Horizontal bars shown above the distributions represent mean locations and the full widths and half maxima. Laurdan and DOPC structures are drawn to scale with the fluorophore located 11.4 Å from the DOPC bilayer center as obtained from parallax quenching [12]. This value depends on the emitted wavelength, which is depicted by the bar with the spectrum of light from 420 to 530 nm; see details in section 3.1.

Fig. 3. Changes of water dynamics around Laurdan molecule in pure water (A) and embedded into DOPC LUVs (B). Maps were plotted as a function of time (abscissa scale) and distance from the chromophore center (ordinate scale). Please note the different scales of the insets. Adapted from [16].

Fig. 4. Mean relaxation time, τ, for Laurdan embedded in DOPC/DOTAP (open squares) or DMPC/DMTAP (open circles) measured at 10°C and 50°C, respectively, and mean area per lipid, $\langle A \rangle$, as calculated by Gurtovenko et al. for DMPC/DMTAP at 50°C (closed circles), adapted from [12, 24]. Both the parameters plotted as a function of cationic lipid molar fraction. Schematic arrangements of lipids for pure PC, PC/TAP (1:1), and pure TAP bilayers, both for DOPC/DOTAP (upper row) and DMPC/DMTAP (lower row), are shown.

Fig. 1

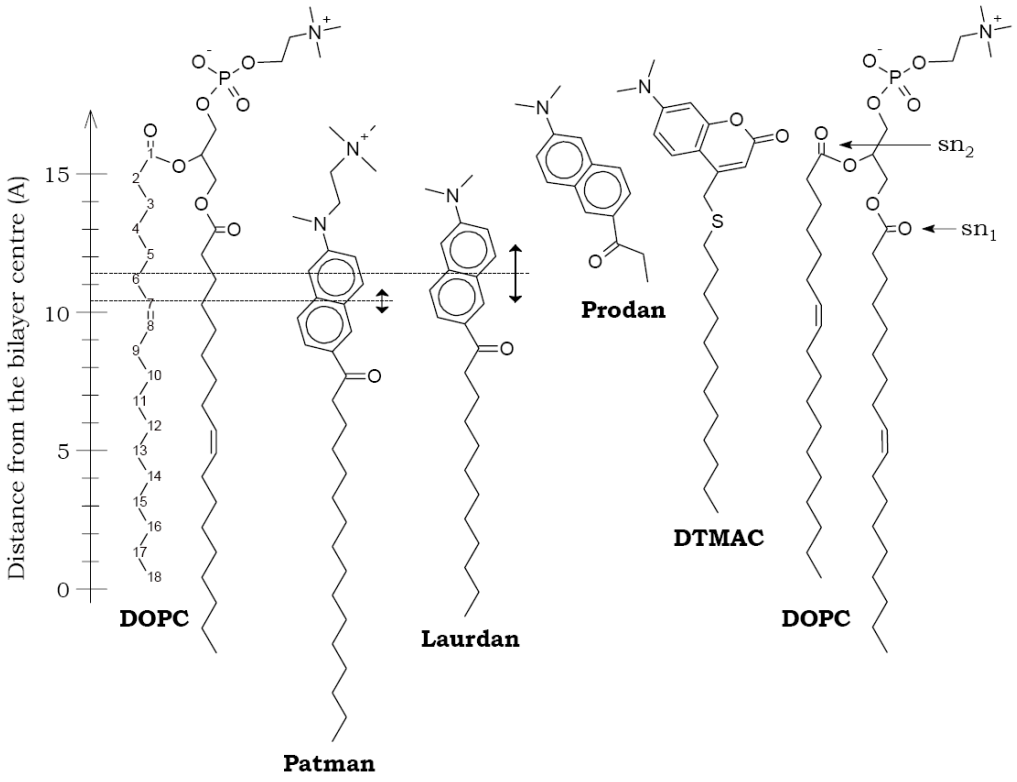
Distance from the bilayer centre (A)
15
10
5
0
DOPC
Patman
Laurdan
Prodan
DTMAC
DOPC
sn2
sn1

Fig. 2

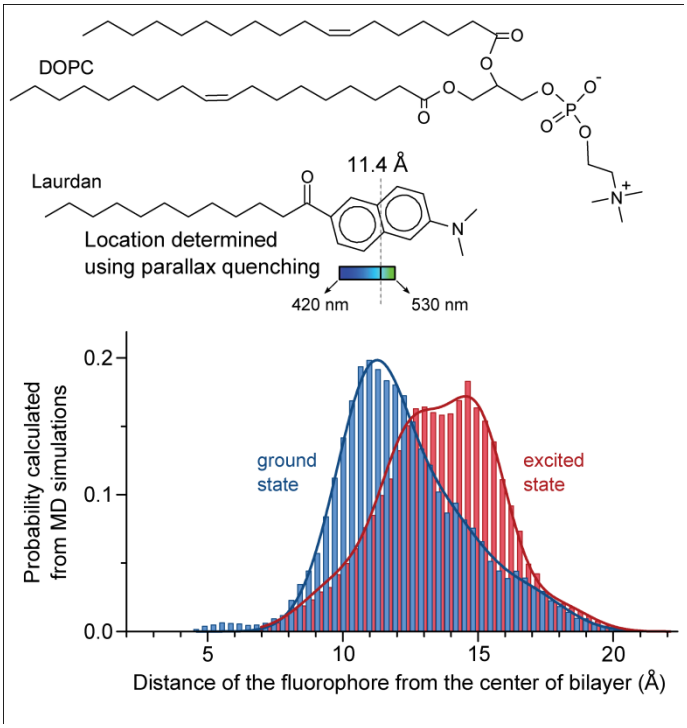
DOPC
Laurdan
11.4 Å
Location determined
using parallax quenching
420 nm
530 nm
Probability calculated
from MD simulations
0.2
0.1
0.0
ground
state
excited
state
5
10
15
20
Distance of the fluorophore from the center of bilayer (Å)

Fig. 3

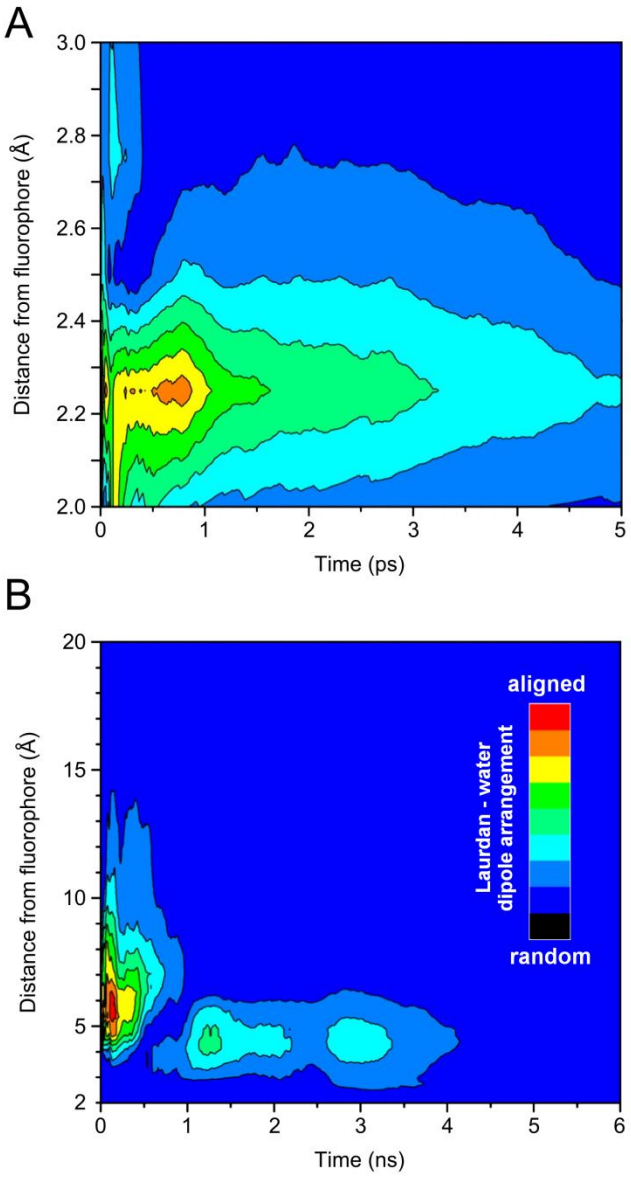
A
3.0
2.8
2.6
2.4
2.2
2.0
Distance from fluorophore (Å)
0
1
2
3
4
5
Time (ps)
B
20
15
10
5
2
Distance from fluorophore (Å)
0
1
2
3
4
5
6
Time (ns)
aligned
Laurdan - water
dipole arrangement
random

Fig. 4

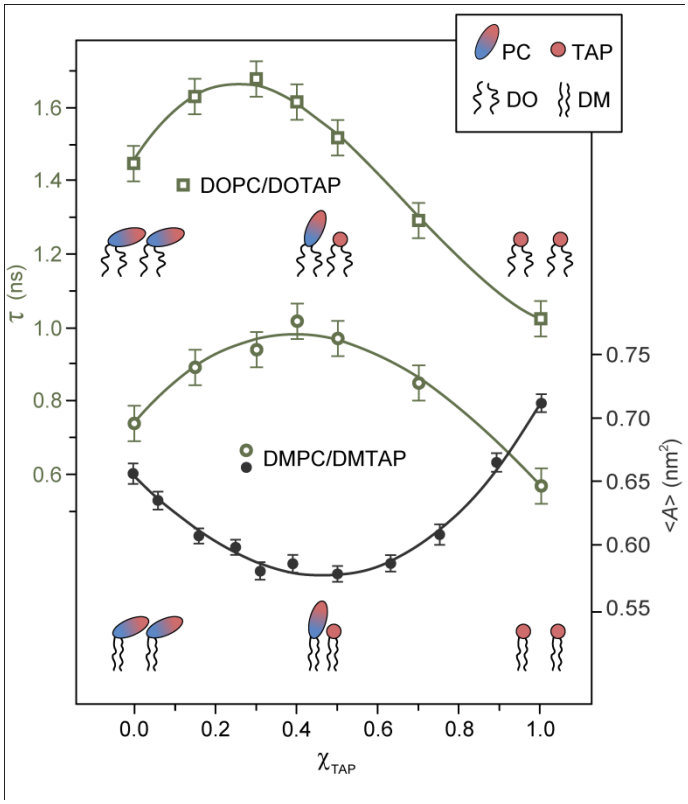
PC
TAP
DO
DM
DOPC/DOTAP
DMPC/DMTAP
τ (ns)
<A> (nm²)
χTAP
1.6
1.4
1.2
1.0
0.8
0.6
0.75
0.70
0.65
0.60
0.55
0.0
0.2
0.4
0.6
0.8
1.0